A Unified Theory of the B-Z Transition of DNA in High and Low Concentrations of Multivalent Ions

M. Guéron,* J.-Ph. Demaret,† and M. Filoche‡

*Groupe de Biophysique de l'Ecole Polytechnique et de Unité mixte de recherche 7643 du Centre National de la Recherche Scientifique, Ecole Polytechnique, 91128 Palaiseau, France; †Laboratoire de Physico-Chimie Biomoléculaire et Cellulaire, Université Pierre et Marie Curie, 75252 Paris Cedex 05, France; and ‡Laboratoire de Physique de la Matière Condensée, UMR 7643 du CNRS, Ecole Polytechnique, 91128 Palaiseau, France

ABSTRACT We showed recently that the high-salt transition of poly[d(G-C)] · poly[d(G-C)] between B-DNA and Z-DNA (at [NaCl] = 2.25 M or [$MgCl_2$] = 0.7 M) can be ascribed to the lesser electrostatic free energy of the B form, due to better immersion of the phosphates in the solution. This property was incorporated in cylindrical DNA models that were analyzed by Poisson-Boltzmann theory. The results are insensitive to details of the models, and in fair agreement with experiment. In contrast, the Z form of the poly[d(G-m5C)] duplex is stabilized by very small concentrations of magnesium. We now show that this striking difference is accommodated quantitatively by the same electrostatic theory, without any adjustable parameter. The different responses to magnesium of the methylated and nonmethylated polymers do not come from stereospecific cation-DNA interactions: they stem from an experimentally derived, modest difference in the nonelectrostatic component of the free energy difference (or NFED) between the Z and B forms. The NFED is derived from circular DNA measurements. The differences between alkaline earth and transition metal ions are explained by weak coordination of the latter. The theory also explains the induction of the transition by micromolar concentrations of cobalt hexammine, again without specific binding or adjustable parameters. Hence, in the case of the B-Z transition as in others (e.g., the folding of tRNA and of ribozymes), the effect of multivalent cations on nucleic acid structure is mediated primarily by nonspecific ion-polyelectrolyte interactions. We propose this as a general rule for which convincing counter-examples are lacking.

INTRODUCTION

Over the past years we have developed simple polyelectrolyte models for understanding the interactions of nucleic acids with ions (Guéron and Weisbuch, 1979, 1980; Weisbuch and Guéron, 1981, 1983; Guéron and Demaret, 1992a), as studied in various laboratories by titrations and by investigations of local properties of the interaction using, for instance, Mn^{2+}-EPR and ^{31}P-NMR (Leroy et al., 1977; Leroy and Guéron, 1977, 1981) and ^{23}Na-NMR (Anderson et al., 1978).

We were led to the conclusion that the association of ions to nucleic acids is mostly electrostatic, and that specific coordination (as found in a metalloenzyme such as zinc-carboxypeptidase) is absent or provides little free energy, so that it is not an important determinant of nucleic acid structure. An example of this situation is provided by tRNA, whose tertiary folded active structure may be formed in the absence of divalent cations, even though such ions induce it efficiently (Guéron and Leroy, 1982). Similarly, the hammerhead ribozyme, which depends on magnesium for catalysis, folds into the active form in the absence of any divalent ion (Heus and Pardi, 1991; Simorre et al., 1997). So does leadzyme, a ribozyme that requires lead for its catalytic function (Legault et al., 1998; Katahira et al., 1998).

A good illustration of nonspecific electrostatic interactions is provided by the equilibrium between the right-handed (B-DNA) and left-handed (Z-DNA) double-stranded helices of poly[d(G-C)]: it is affected by solute ions such as Na^+ and Mg^{2+}, and the concentrations required to drive the transition at room temperature are large (respectively 2.5 and 0.7 M of the chloride salt, corresponding to similar ionic strengths), suggesting that the effects are in good part nonspecific (Pohl and Jovin, 1972). From the concentration required to drive the transition in DNA fragments of different lengths, one can derive the *variation* of the free energy difference (FED) with ionic strength (Pohl, 1983). This provides a direct test of electrostatic theories (Frank-Kamenetskii et al., 1985), the only test that is independent of *non*electrostatic contributions to the free energy difference, designated henceforth as NFED.

Previously, we used this test to validate a simple Poisson-Boltzmann model of the interactions between ions and DNA. B-DNA and Z-DNA were represented by composite cylinders whose penetrability to water and ions reflects the main electrostatic difference between them: the *better immersion of the charged phosphate groups of B-DNA* into the solution, resulting in their better screening by counterions (Fig. 1).

The model approximately reproduces the experimental variation of the FED versus salt concentration (Guéron and Demaret, 1992b; Demaret and Guéron, 1993). This success shows that the electrostatics of nucleic acid solutions may be understood simply, in a theory that treats the solvent as continuous, which ignores any specific interactions between DNA and ions and whose predictions are insensitive to the

Received for publication 27 September 1999 and in final form 2 November 1999.

Address reprint requests to M. Guéron, BIOP, Ecole Polytechnique, 91128 Palaiseau, France. Tel.: 33-1-6933-4412; Fax: 33-1-6933-3004; E-mail: mg@pmc.polytechnique.fr.

0006-3495/00/02/1070/00 $2.00

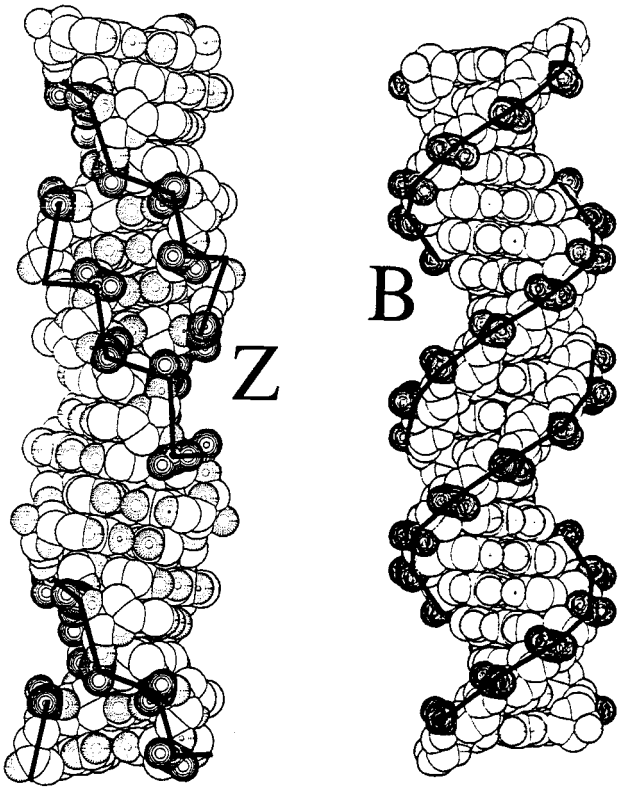

FIGURE 1 The structures of Z-DNA and B-DNA. The sugar-phosphate backbone is marked by the heavy line, and the atoms of the phosphate group are emphasized. In the B-DNA structure, the phosphates jut out into the solution, whereas in Z-DNA they are held much closer to the rest of the DNA matter. Therefore, screening of the DNA charge by counterions is more efficient in the B form. After Wang et al. (1979), with permission.

choice of ionic radius or to the details of DNA structure provided that the main features (here, the different immersion of the phosphates in the B and Z forms) are taken into account. The results are also in agreement with a Poisson-Boltzmann calculation that represents the DNA structures in atomic detail (Misra and Honig, 1996).

The difference in the immersion of phosphates is essential. When B-DNA and Z-DNA are described in terms of their sole linear charge, one finds no B to Z transition in high salt (Manning, 1978; Fenley et al., 1990); when they are modeled as nonporous cylinders differing only by their radius and linear charge density, Poisson-Boltzmann theory either makes the same prediction or fails quantitatively (Frank-Kamenetskii et al., 1985).

Good rendering of electrostatic properties is only as important as these properties themselves. Is electrostatics important for the physical chemistry of nucleic acids? Or do the interesting features of DNA-ion interactions lie beyond electrostatics? Again, the B-Z transition provides a good opportunity to examine this question, inasmuch as *the effect of multivalent ions on the B-Z transition is a challenge for any electrostatic theory*. This is summarized in the six entries of Table 1 (Behe and Felsenfeld, 1981), whose diversity seems incompatible with simple electrostatics.

Indeed, whereas the effect of sodium on the B-Z equilibrium is comparable for the methylated and nonmethylated species (as stated above), the effect of magnesium is completely different, since magnesium drives the B-Z transition of the methylated species at concentrations of 0.6 mM, in sharp contrast to 700 mM for the nonmethylated species! As for trivalent cobalt hexammine, it drives the transition to the Z form at micromolar concentrations, lower by orders of magnitude than the critical concentrations of the monovalent and divalent cations. For reference, one notes that in the linear (Debye-Hückel) theory, electrostatic properties are determined by the ionic strength (Eq. 4), so that the concentrations of magnesium and cobalt hexammine equivalent to 2500 mM sodium chloride would be 830 and 415 mM, respectively.

At first sight, it seems that a common electrostatic explanation of the observations is impossible and that nonelectrostatic effects are involved, for instance specific binding of Mg^{2+} to a Z-form site present in the methylated species, but not in the nonmethylated one. Similarly, the effect of cobalt hexammine at micromolar concentrations might be considered evidence enough for specific binding sites. These observations and others may lead one to the assumption that the chemistry of the cation, the details of spacing between phosphates, and/or interionic correlations play an important role in the B-Z transition (Behe and Felsenfeld, 1981; Chen et al., 1984; Klement et al., 1991; the latter work is discussed in Guéron and Demaret (1992b) and in Demaret and Guéron (1993)).

The primary goal of the present work is to show that the effects of ions described in Table 1 may be understood in the Poisson-Boltzmann model of strongly charged polyelectrolytes in terms of the ionic distribution in mixed salt solutions (Weisbuch and Guéron, 1981), and without invoking any specific interactions. To this end, one must consider the absolute value of the total FED, rather than its sole variations as a function of salt. Experimental values of the total FED are available. When they are introduced in the theory (with no adjustable parameter), one finds that the modest difference between the nonelectrostatic contributions to the FED of the methylated and nonmethylated species provides a semi-quantitative explanation of the features in Table 1. The model also accounts for other properties of the competition between counterions of different

TABLE 1 Ionic concentrations for the B-Z transition (mM)

	Na^+	Mg^{2+}	$Co(NH_3)_6^{3+}$
poly[d(G-C)]	2500	700	0.030
poly[d(G-m^{5}C)]	700	0.6	0.003

At room temperature. The magnesium and cobalt hexammine solutions also contain NaCl, 50 mM. DNA concentration is 0.01 mM (in phosphate). Data are from text and Fig. 5 of Behe and Felsenfeld (1981).

valencies, such as the observed invariance of the composition of the counterion sheath at the transition (Chen et al., 1984), or the disproportionate effect of fractional methylation. The theoretical results are presented as graphs that provide a straightforward explanation of the multiple observations concerning the effect of ions on the B-Z transition.

More generally, this work shows how a low concentration of multivalent ions can influence the structure of nucleic acids even in the absence of any specific, high-affinity site. It should help researchers distinguish between the powerful and somewhat subtle effects of nonspecific electrostatic interactions and those resulting from strong specific interactions between ions and nucleic acids, if they exist. The same analysis should apply to highly charged membranes.

THE B-Z TRANSITION: SELECTED EXPERIMENTAL RESULTS

The B-Z transition of poly[d(G-C)] and poly[d(G-m^{5}C)] in single-salt solutions

In $NaClO_4$ solution at 22°C, poly[d(G-C)] converts to the Z form at a salt concentration of ~2.25 M. From the transition concentration versus DNA length, one derives the FED per phosphate, $F_Z - F_B$, of the infinite polymer for salt concentrations between 1.5 and 4.8 M (Pohl, 1983). The FED includes both electrostatic and nonelectrostatic contributions, but its *variation* versus salt is considered purely electrostatic, and it may therefore be compared with the prediction of electrostatic theories.

In $MgCl_2$ solution the transition concentration is 0.7 M instead of 2.25 M in NaCl (Behe and Felsenfeld, 1981), so that the ionic strength at the transition is nearly the same in the two cases. Upon increasing the temperature, the critical Mg^{2+} concentration decreases slowly at first, down to ~0.1 M at 60°C (Behe et al., 1985). However, at higher temperatures the decrease accelerates, so that above 75°C Z-DNA becomes the stable form of the Mg^{2+} salt of poly[d(G-C)], even at the lowest magnesium concentrations (Fig. 2 *a*).

The addition of alcohol (Behe and Felsenfeld, 1981; van de Sande and Jovin, 1982) affects the transition similarly to an increase in temperature, as do bromination or methylation of cytidine. Indeed, the behavior of poly[d(G-m^{5}C)] at room temperature resembles that of poly[d(G-C)] above 75°C in water, or at room temperature in mixed alcohol/water solvent: there is a B → Z transition when the $NaClO_4$ concentration increases to 0.7 M; and the stable form in pure magnesium solution is Z-DNA for all magnesium concentrations.

Negative supercoiling is another process that stabilizes the Z form (Singleton et al., 1982; Stirdivant et al., 1982; Peck and Wang, 1983; Zacharias et al., 1988). One can use it to determine the free energy surplus of the Z form over the B form. In 0.1 M monovalent salt at room temperature, this is 0.32 kcal/basepair for poly[d(G-C)] and 0.11 kcal/base pair for poly[d(G-m^{5}C)] (Zacharias et al., 1988), equivalent to 0.67 and 0.23 kJ/phosphate, respectively.

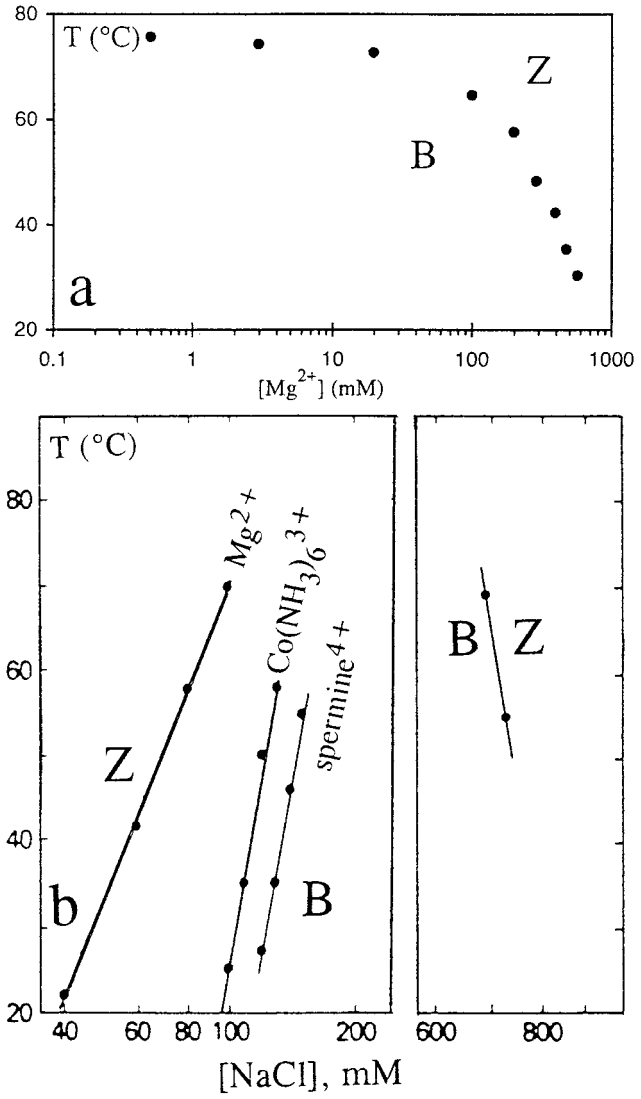

FIGURE 2 (a) Temperature of the B-Z transition of poly[d(G-C)] as a function of magnesium concentration. Above 75°C, Z-DNA is the stable form of the magnesium salt of DNA. (*b*) The B-Z transition of poly[d(G-m^{5}C)] in mixed salt (*left panel*), and from Z-DNA to B-DNA in pure monovalent salt (*right panel*). From left to right, the data in the left panel correspond to: Mg^{2+}, 500 μM; cobalt hexammine^{3+}, 20 μM; spermine^{4+}, 10 μM. These are TOTAL (not free) concentrations. The DNA phosphate concentration is 50 μM. Note the contrast between the two panels. Increasing sodium favors the B form at left, the Z form at right. In both panels an increase in temperature favors the Z form, and this corresponds to opposite slopes in the two panels. After Behe et al. (1985), with permission.

The B-Z transition in mixed salt

The effect of the ionic composition of the solution on the B-Z transition has been extensively studied. A good example is provided in Fig. 2 *b*, which plots the temperature of the B-Z transition in poly[d(G-m^{5}C)] as a function of mono-

valent salt concentration in solutions of various salt compositions (Behe et al., 1985).

The full lines on the left correspond to mixed salt solutions, including a fixed concentration of a multivalent cation. The transition for increasing sodium is from the Z form to the B form. The positive, but steep, slope versus temperature indicates that the Z form is favored, but slightly, at high temperatures.

The right panel corresponds to pure sodium chloride solutions. In contrast to the mixed-salt case, the transition for increasing sodium is from B to Z, and the B form is favored at high temperature, as shown by the negative slope.

In a variation of the mixed-salt experiment, one starts with a solution of B-DNA in monovalent salt, and the B to Z transition is induced by the addition of multivalent cations. If the DNA phosphate concentration is small compared to the total multivalent ion concentration at the transition, the experiment provides the *concentration of free multivalent ions* at the transition. This is the situation for the measurements corresponding to the two highest potassium concentrations in Fig. 3 *a*.

In the case of the lowest potassium concentration (0.6 mM), the total concentration of magnesium at the transition is much lower than the DNA concentration (0.1 mM in phosphate) and most of the magnesium is in the sheath. The free magnesium concentration is therefore unknown, but the experiment does provide the *sheath composition* at the transition, where the sheath is defined as the region around the polyelectrolyte that contains the neutralizing charge; its composition is characterized by the number, or by the charge, of multivalent ions in the sheath, per phosphate. In the case of magnesium and poly[d(G-m^{5}C)], there is 0.1 magnesium in the sheath per phosphate at the transition, so that 20% of the charge is neutralized by divalent ions (Chen et al., 1984).

Fig. 3 *b* provides data for the B-Z transition in a mixture of $Co(NH_3)_6^{3+}$ and Na^+ cations. At high ionic concentrations, the plot of the critical concentration of trivalent versus monovalent ion is a straight line whose slope is close to 3, as expected in the electrostatic theory (see below). The point at 100 mM sodium and 20 μM cobalt hexammine is in agreement with the data in Fig. 2 *b*. In low sodium, the plots for different DNA concentrations become distinct because most of the trivalent cation is in the sheath, so that the total concentration (plotted) differs from the much smaller free concentration that is the proper thermodynamic variable. Each plot is now a horizontal line, showing that the number of trivalent cations in the sheath at the B-Z transition is independent of the monovalent salt concentration. This number is 0.023 per phosphate, so that trivalent ions account for the neutralization of a fraction 0.07 of the charge.

These measurements provide two important and contrasting results. First, the concentrations of free divalent and trivalent ions required to drive the B to Z transition differ strongly: for instance, in poly[d(G-m^{5}C)] at a monovalent

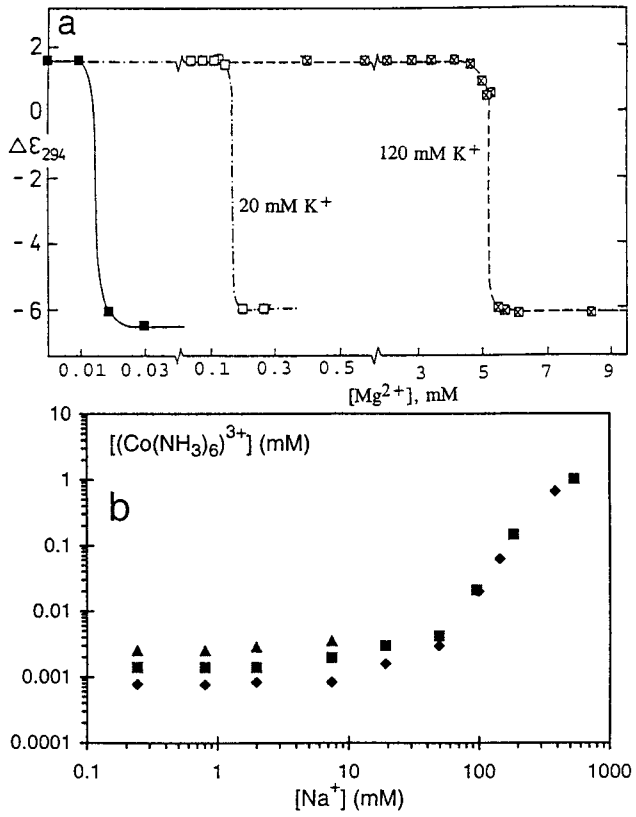

FIGURE 3 The B-Z transition of poly[d(G-m^{5}C)] in mixed salt solutions, as observed by circular dichroism (see also Fig. 9). (*a*) In Mg^{2+}/K^+ solution (after Sági et al. (1991), with permission). From left to right the transitions correspond to 1.2, 20, and 120 mM potassium. The abscissa is the total concentration of magnesium. The DNA phosphate concentration is ~0.1 mM. In the case of the 1.2 mM potassium transition, total and free Mg^{2+} differ strongly. (*b*) In $Co(NH_3)_6^{3+}/Na^+$ solution (after Chen et al. (1984), with permission). Here also, the plot is of total, rather than free, ionic concentrations. For the points at left, nearly all of the cobalt hexammine is in the DNA sheath, and the ratio of cobalt hexammine to DNA phosphate at the transition is 0.025, independently of DNA concentration (◆, 35 μM; ■, 70 μM; ▲, 140 μM). At right, most of the cobalt hexammine is free, and the log-log plot is a straight line with slope 2.85.

salt concentration of 50 mM, the *critical concentrations* are 600 and 3 μM, respectively, for Mg^{2+} and $Co(NH_3)_6^{3+}$ (Table 1). Second, in the same conditions, the *critical fractions* of counterionic charge contributed to the sheath by the multivalent ion differ much less, being 0.20 and 0.07, respectively. We shall see that it is the charge fraction in the sheath, rather than the free ion concentration, which is related to the free energy.

THEORY

Earlier, we created porous cylinder models of B-DNA and Z-DNA (Fig. 2 in Demaret and Guéron, 1993). The models are the cylindrical average of the distributions of B-DNA and Z-DNA matter; of the complementary space, accessible to the (small) water molecules, where the dielectric constant

is set at 80; and of the space accessible to solute ions, with a single ionic radius, that of hydrated Na^+ (0.235 nm). The charge of phosphate oxygens is uniformly spread out on two cylindrical surfaces of appropriate radii. The porous cylinders were simplified to composite cylinders, for which we solved the Poisson-Boltzmann equation and computed the electrostatic free energy, with application to the B-Z transition in pure salt. In the present work we apply the porous cylinder models to the B-Z transition in mixed salt (Figs. 7 and 8). For convenience, we include a summary of previous results.

Poisson-Boltzmann theory of DNA cylindrical models: the planar approximation

DNA may be modeled by cylinders of circular section, with, in the simplest case, a single uniform charge layer at the surface. Numerical solutions of the Poisson-Boltzmann equation show that the electrostatic properties (counterion distribution, electrostatic potential, and free energy) are close to those of a plane with the same superficial charge density as the cylinder, provided that the curvature radius of the cylinder is larger than the scaling length for the variation of the electric field near the cylinder surface. This condition is expressed by the same relation as that defining highly charged cylinders: $\xi > 0.5/z$, where ξ is the linear charge density parameter and z is the cationic charge (Weisbuch and Guéron, 1983). This definition differs slightly from that of condensation theory (Manning, 1969). B-DNA and Z-DNA are indeed highly charged cylinders, with ξ values of 4.2 and 3.9.

In the planar approximation, the Poisson-Boltzmann problem is easily solved. There is a solution in closed form for the case of a plane in single salt. The planar approximation is often sufficiently accurate for the study of the cylinder. If not, it is a good guide for the development of approximate algebraic formulas or of numerical methods (Weisbuch and Guéron, 1981).

Models of B-DNA and Z-DNA: the electrostatic free energy in pure salt

The major geometric difference between B-DNA and Z-DNA with regard to electrostatic properties is that the phosphates jut out in the B form, so that they are well surrounded with water and ions, whereas in the Z form they are quite close to the rest of the DNA matter (Fig. 1). One might also say that the surface of B-DNA is corrugated, whereas that of Z-DNA is relatively smooth.

In a crude model of this difference, B-DNA is represented by a hollow cylinder with solution both inside and outside its charged surface, and Z-DNA by a cylinder with solution on the outside only. We presently neglect the difference in the surface charge density, σ, between the two cases. In the planar approximation, B-DNA becomes a charged plane immersed in solution on both sides, while Z-DNA is a charged plane with solution on only one side (Guéron and Demaret, 1992b). The free energy F_{one} of a plane immersed on one side is given by:

$$zF_{one}(\sigma, \lambda)/(2kT) = \text{arcsinh}(1/x) + x - (1 + x^2)^{0.5} \quad (1)$$

with

$$x = \text{TH}/\lambda \quad (2)$$

$$\text{TH} = 1/(2\pi l_B z\sigma/e) \quad (3)$$

where l_B is the Bjerrum length $e^2/(4\pi\epsilon_0 DkT)$, ϵ_0 and D being the absolute and relative dielectric constants. The Bjerrum length is 0.72 nm in water at room temperature. For a highly charged surface in low salt (nonlinear regime), TH is the scaling length for the variation of the electric field at the surface, and it also describes the *thickness* of the ionic sheath near the surface. For B-DNA, represented by a charged cylinder of radius 0.95 nm, Eq. 3 gives in monovalent salt: TH = 0.226 nm.

The Debye length, λ, is given by:

$$\lambda^{-2} = 4\pi l_B \Sigma n_i z_i^2 = 4\pi l_B I \quad (4)$$

where n_i and z_i are the valency and concentration of ion i, and I is the ionic strength. In monovalent salt, λ (nm) = $(10.8\ c)^{-1/2}$, where c is the salt concentration in mol/l. In the linear regime, the scaling length is equal to λ.

It follows from Eqs. 2–4 that TH/λ in pure salt at a given concentration is independent of z, the salt valency. The free energy of the plane has the following properties. 1) In z-valent salt, it is equal to $1/z$ times the free energy in monovalent salt at the same concentration; 2) for small x (low salt, nonlinear regime), the leading terms in Eq. 1 are:

$$zF_{one}(\sigma, \lambda)/(2kT) = \log(1/x) - 1/2 + x$$
$$= \log(\lambda) - \log(\text{TH}) - 1/2 + \text{TH}/\lambda; \quad (5)$$

and 3) for large x (high salt, linear regime), the leading term is:

$$zF_{one}(\sigma, \lambda)/(2kT) = 1/(2x) = \lambda/(2\text{TH}) \quad (6)$$

The free energy for a plane immersed on both sides, F_{two}, is equal to that of a plane immersed on one side, F_{one}, having half its charge density. The electrostatic free energy difference, $F_Z - F_B$, is then $F_{one}(\sigma) - F_{one}(\sigma/2)$. In low salt, it is independent of σ and of salt concentration according to Eq. 5, where the last term is negligible. In high salt, it varies as $\sigma/c^{1/2}$. In both cases, it is inversely proportional to the salt valency.

Fig. 4 is a plot of the electrostatic free energy difference (EFED) computed with the porous cylinder models of the real distributions of matter and charge in B- and Z-DNA. The main features are the same as in the planar model. However, the EFED decreases slowly as the salt concentration is reduced, rather than remaining constant. And the dependence of the low-salt EFED on salt valency is weaker than the factor $1/z$.

In the present work we use the planar model as a guide, but all computations are carried out with the porous cylinder models unless stated otherwise. We do not distinguish between the structures of poly[d(G-C)] and poly[d(G-m^{5}C)],

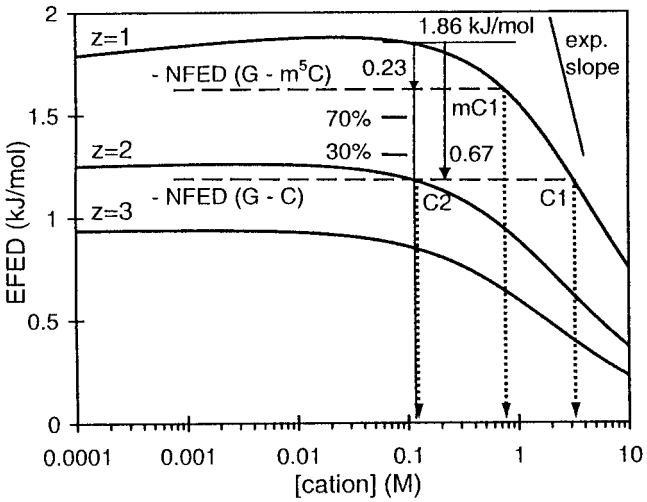

FIGURE 4 The Poisson-Boltzmann electrostatic free energy difference (EFED) (free energy of Z-DNA minus that of B-DNA, per phosphate) in solutions of a single salt, for valencies $z = 1, 2, 3$. The variation in high salt corresponds to Debye screening. The theoretical slope in monovalent salt is in fair agreement with the experimental one for poly[d(G-C)] (Pohl, 1983), plotted as "exp. slope" at the appropriate salt concentrations, and at an arbitrary vertical position (Demaret and Guéron, 1993). In low salt the EFED is nearly independent of salt concentration in relation to the near-constancy of the counterion distribution. All computations in this work use the porous cylinder DNA models (see text), with ionic radii of 0.235 nm. The horizontal lines correspond to a salt-independent nonelectrostatic free energy difference (NFED). The −NFED value is such that the total FED, (EFED − (−NFED)), is equal to that determined in the supercoiling experiments of Zacharias et al. (1988), in 0.1 M NaCl; 0.23 and 0.67 kJ/phosphate for the methylated and nonmethylated species, respectively. The markers labeled 30% and 70% are the linearly interpolated −NFED values for partially methylated species (see text). The pure salt concentrations for the B-Z transition are predicted to occur at points C1 and C2 for poly[d(G-C)] in monovalent and divalent salt, respectively. For poly[d(G-m^{5}C)], the transition in monovalent salt is predicted at point mC1, corresponding to C1 of poly[d(G-C)]. But there is no point mC2 (corresponding to C2). Therefore, the graph predicts that in pure divalent salt the stable form of poly[d(G-m^{5}C)] is Z-DNA, whatever the salt concentration, as is indeed observed. The near-coincidence between the value of −NFED for poly[d(G-C)] and the maximum EFED in divalent salt implies drastic effects of a slight increase of −NFED (such as caused by a change in temperature or by partial methylation) on the B-Z transition of poly[d(G-C)] in a divalent ion solution, in contrast to solutions of monovalent or trivalent ions. Fig. 2*a* may be interpreted in this manner (see text).

and the EFED is therefore the same for both. The properties of the B-Z transition discussed below, and particularly the effect of multivalent ions, follow from the elementary features of the EFED displayed in Fig. 4.

The nonelectrostatic free energy difference (NFED)

The transition between the B and Z forms takes place when the FED between the two forms is zero. The FED is the sum of the electrostatic contribution, EFED, and of other contributions, which are related to differences between the two forms in stacking free energy, in hydrogen-bonding to solvent, in dipolar interactions with solvent, etc. These contributions may depend on the chemical nature of the nucleic acid (base sequence, methylation, etc.), on the composition of the solvent (e.g., water-alcohol mixture), and on the temperature; but they should be approximately independent of the nature, valency, and concentration of the salt. They constitute the nonelectrostatic contribution, or NFED.

The NFED turns out to be negative: in other words, the Z form is more stable than the B form, except for electrostatics. This fits with the general observation of a transition to the Z form in high salt, i.e., in conditions where screening brings down the electrostatic contribution to free energy.

For a graphical description, we note that the (total) FED is equal to EFED minus (−NFED). The −NFED values are determined by the condition that the FED in 0.1 M salt must match that measured by Zacharias et al. (1988) at room temperature, 0.67 and 0.23 kJ/phosphate for poly[d(G-C)] and poly[d(G-m^{5}C)], respectively (see "Selected experimental results" above). Fig. 4 includes horizontal lines for the corresponding −NFED values, 1.19 and 1.63 kJ/phosphate.

At each salt concentration the FED is equal to the distance between the EFED curve and the −NFED line. It is zero at their intersection. For poly[d(G-C)], there are intersections with the EFED curves for mono and divalent ions, at points C1 and C2, corresponding to B-Z transitions in each of these pure-salt cases. But there is no intersection with the EFED for trivalent ions, therefore the Z form is stable in solutions of trivalent cations at any concentration. For poly[d(G-m^{5}C)], the intersection of the horizontal with the EFED curve (point mC1) indicates a B-Z transition at 0.75 M pure monovalent salt, in agreement with observations (Fig. 2 *b, right-hand panel*; Table 1). There is no intersection with the divalent EFED curve, hence the Z form is stable in pure divalent salt for all concentrations (and also in pure trivalent salt), as observed (Behe and Felsenfeld, 1981).

We thus obtain an important result: *a modest shift of the nonelectrostatic FED (the NFED) radically changes the behavior of the B-Z equilibrium in a solution of divalent cations.* In one case, the Z conformation occurs only at high divalent salt concentration, whereas in the other case this

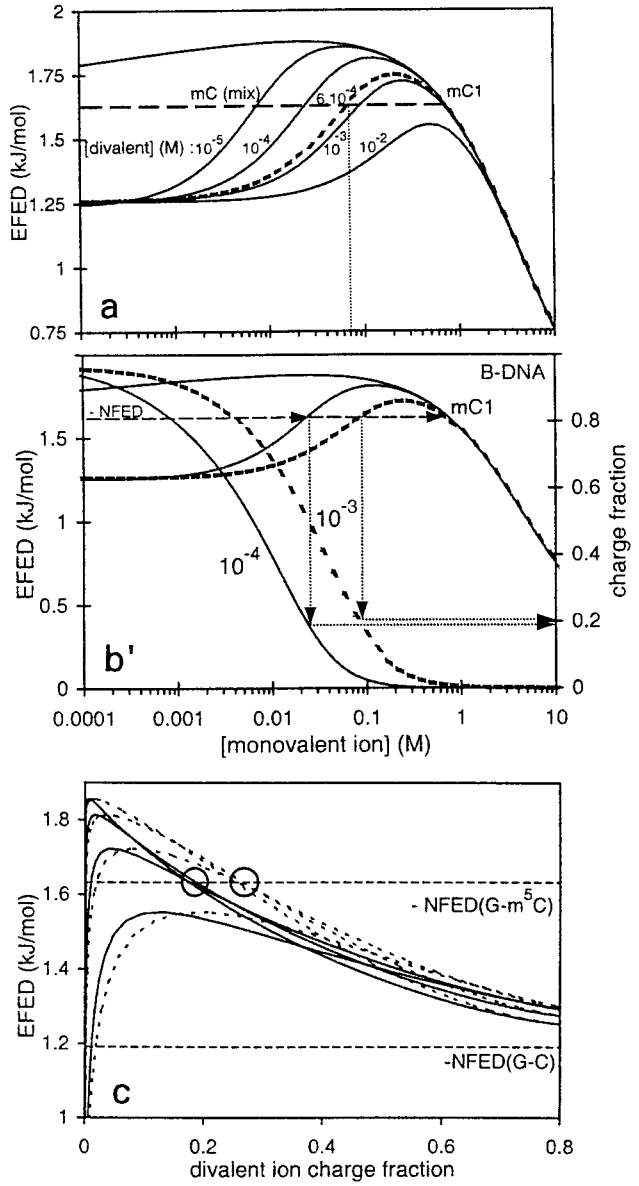

FIGURE 5 (*a*) The EFED curves, as a function of monovalent cation in mixed salt, for different concentrations of divalent ions, as labeled. In low monovalent salt, the EFED is close to that in pure divalent salt. In high salt, it changes to the monovalent ion values. The horizontal line is the (−NFED) line for poly[d(G-m^{5}C)]. It crosses each EFED curve (except for the 10^{-2} M curve) at two points. The monovalent ion concentration at the low-salt Z to B transition, mC(mix), is approximately proportional to the square root of the divalent ion concentration. The monovalent ion concentration at the high-salt B to Z transition is nearly the same for the different divalent ion concentrations, quite close to the transition point in pure monovalent salt, at mC1. The EFED curve in pure monovalent salt is also shown (same as in Fig. 4). The dashed curve represents −EFED at a divalent ion concentration of 0.6 mM, for comparison with the magnesium data in Table 1. The transition occurs for a monovalent cation concentration of 68 mM. (*b′*) Comparison of the EFEDs in mixed salt for 10^{-4} and 10^{-3} M divalent cations, together with the charge fraction (*right-hand Y scale*) of divalent cations *in the sheath of B-DNA* (not as Fig. 6 *b″*). The charge fraction at the B-Z transition is determined by a graphical construction, as indicated. It is nearly the same for the two concentrations of divalent ions. (*c*) The EFED as a function of the charge fraction for B-DNA (*solid lines*) and Z-DNA (*dashed lines*). Each line corresponds to a given concentration of divalent ions. The concentrations are those of (*a*) except for the $6 \cdot 10^{-4}$ M concentration. They increase in order of decreasing maximum EFED. The intersection with the −NFED horizontal dashed line corresponds to the B-Z transition. The charge fraction is nearly independent of the divalent ion concentration for all concentrations up to 10^{-3} M. The charge fraction is larger for Z-DNA than for B-DNA, and the average is 0.24.

conformation is the stable one for all divalent salt concentrations. Fig. 4 shows that this property is related to the near-constancy of the electrostatic FED (the EFED) in low salt. In turn, this originates directly in the logarithmic dependence of the electrostatic free energy on salt concentration for highly charged surfaces (Eq. 5).

The B-Z transition in mixed salt

We consider DNA in solutions with a fixed concentration, n_2, of divalent cations (Mg^{2+}) and with variable concentrations, n_1, of Na^+. When the NaCl concentration is low enough, the DNA sheath contains mostly Mg^{2+}, and the EFED is close to the value in pure divalent salt. Higher Na^+ concentrations displace Mg^{2+} from the sheath, and the EFED increases, finally connecting to the monovalent salt values.

The variation of EFED is shown in Fig. 5 *a*. The transition curves for different concentrations of divalent cation have similar shapes. A translation along the *x* axis corresponding to a 10-fold increase in n_1 brings into near-coincidence the curves that correspond to a hundredfold change in n_2. Thus, the EFED is the same in mixed-salt solutions having the same value of n_2/n_1^2: selectivity for divalent ions increases strongly at low monovalent ion concentrations. The figure shows that for a divalent concentration of $6 \cdot 10^{-4}$, the transition takes place at 68 mM monovalent cation concentration, quite close to the experimental value, 50 mM sodium, in Table 1 (also see Fig. 9).

Fig. 5 *b′* shows the fraction of the neutralizing charge in the sheath of B-DNA (per phosphate) contributed by divalent ions at two concentrations, as a function of monovalent salt. Also shown is the construction that gives the charge fraction at the B-Z transition. It is nearly identical (0.18) for the two concentrations. The graph for Z-DNA would be similar, but the charge fraction would be somewhat larger, as described below (Fig. 6 *b″*).

Fig. 5 *c* shows the charge fraction as a function of EFED. Each line corresponds to one divalent cation concentration. The B-Z transition occurs when EFED is equal to − NFED, a value indicated by a horizontal dashed line. For methylated DNA, the charge fraction is nearly independent of divalent cation concentration for all multivalent cation concentrations (highlighted by a circle), except very large ones: the composition of the sheath at the transition is the same

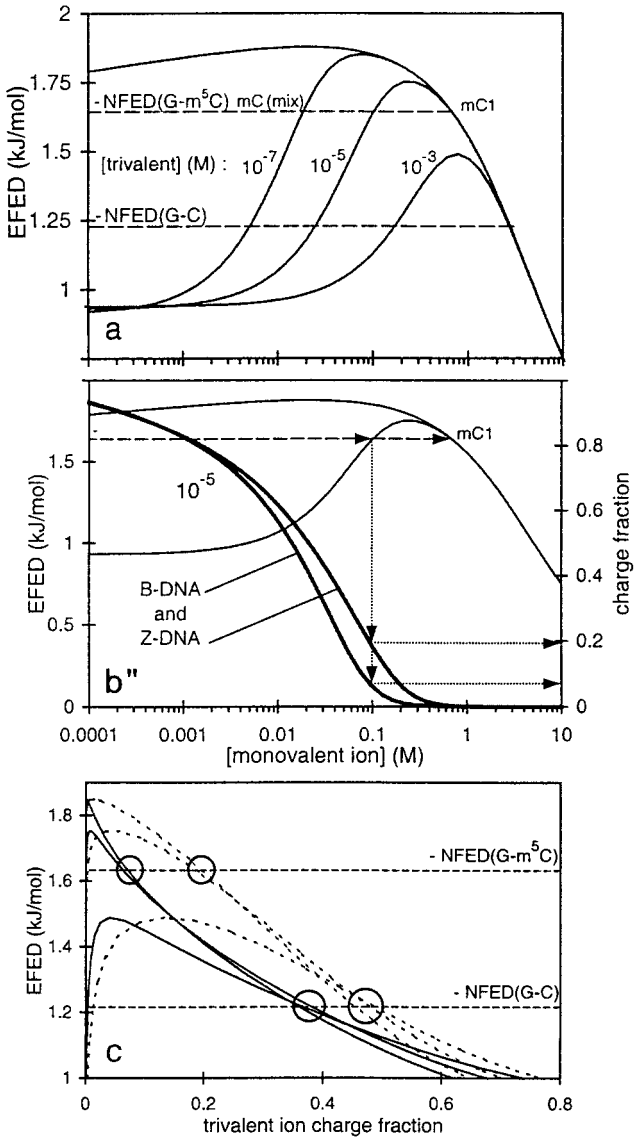

FIGURE 6 The EFED in mixed trivalent/monovalent salt. This is a companion figure to Fig. 5. (*a*) The trivalent salt concentrations are 10^{-7}, 10^{-5}, and 10^{-3} M. (*b″*) Comparison of the EFEDs in mixed salt for 10^{-5} M trivalent ions, together with the charge fraction (*right-hand Y scale*) of these cations *in the sheaths of B-DNA and Z-DNA* (not as Fig. 5 *b′*). The charge fraction is much larger for Z-DNA (0.19) than for B-DNA (0.06). (*c*) The EFED as a function of the charge fraction. The circles pinpoint the values for Z-DNA and B-DNA, for the methylated and nonmethylated polymers.

for all mixed salt solutions, and the sheath of Z-DNA is richer in divalent cations than that of B-DNA. The −NFED line for nonmethylated DNA does not cross the EFED curves, as expected from the general configuration of Fig. 4.

The properties of mixed trivalent/monovalent salt solutions are presented in Fig. 6. The middle panel (6 *b″*) displays the different charge fractions for the B and Z forms for a single trivalent ion concentration. The bottom panel shows that, as with divalent ions, the critical charge fractions (i.e., those corresponding to the B-Z transition) are nearly independent of the multivalent ion concentration for the methylated and nonmethylated polymers.

The larger charge fraction contributed by divalent ions for Z- than for B-DNA at the B-Z transition is required by Le Châtelier's principle on the displacement of equilibrium, since addition of divalent ions favors the Z form. This is directly related to the geometrical difference between the two forms: the corrugated surface of B-DNA provides better screening of the phosphate charge than the smoother surface of Z-DNA, hence the B-DNA surface potential is lower, and so is the selectivity for divalent ions. Titration measurements provide only the average charge for the two forms, and we are not aware of any spectroscopic measurements aimed at measuring the two fractions separately. Such measurements would test the present analysis, which is the first to separately provide the charge fraction of each form.

To summarize, the theory makes four main predictions concerning DNA in mixed salt:

1. The critical *z*-valent cation concentration is proportional to the *z* power of the monovalent concentration;
2. The critical sheath composition is independent of the chosen multivalent salt concentration;
3. The critical sheath composition is affected by factors such as the temperature, or cytidine methylation, which change the NFED;
4. In all conditions, the sheath of Z-DNA is richer in multivalent ions than that of B-DNA.

These properties of the porous cylinder model agree with the observations in "B-Z transition in mixed salt," and a quantitative comparison will be given below. As noted above, they are closely similar to those of highly charged planes, which therefore provide a qualitative understanding of the general features of the ionic distribution and of the electrostatic free energy (Guéron and Demaret, 1992b). For instance, the Grahame sum rule (Grahame, 1947; Weisbuch and Guéron, 1981) states that in the case of a plane the sum S of concentrations in the immediate vicinity of the surface (or CIV) is independent of the ionic concentrations at large. In the case of DNA models, S is in the range of a few mole/liter. Furthermore, for a counterion whose valency is z and whose concentration is n_z:

$$\mathrm{CIV}_z/n_z = \exp(zV_0/kT) \tag{7}$$

where V_0 is the potential at the polyelectrolyte surface. Hence,

$$\mathrm{CIV}_z/n_z = [\mathrm{CIV}_1/n_1]^z \tag{8}$$

If we consider conditions where most of the sheath ions are monovalent, so that $\mathrm{CIV}_1 \approx S$, we have

$$\mathrm{CIV}_z = n_z[S/n_1]^z \tag{9}$$

which shows that the concentration of z-valent ions required for generating a given value of CIV_z is proportional to the z power of the monovalent ion concentration, as in property 1 stated above. An approximate expression for the composition of the sheath is easily derived from Eq. 9 (Weisbuch and Guéron, 1981).

Computation procedures and results

To avoid convergence problems we resorted to a finite element procedure. The integration proceeded directly from the cylinder axis, through the porous cylinder and its charged layers, and up to a large distance, 500 nm. The number of elements was 13,000.

As an example, Fig. 7 *a1* is a plot of the porosity of B-DNA, i.e., the volume fraction accessible to the solute ions (Demaret and Guéron, 1993), and of the B-DNA electrostatic potential in 50 mM monovalent salt, versus the distance from the cylinder axis. In Fig. 7 *a2* we plot the cylindrical excess charge densities of sodium and chloride ions, per phosphate, so that the sum of the areas under the curves is equal to 1. Fig. 7 *b* shows the ionic charges in mixed salt, for sodium and magnesium concentrations of 50 mM and 0.1 mM, respectively. Magnesium is preferentially concentrated in the inner region and contributes ~7.3% of the neutralizing charge.

Fig. 8 shows corresponding results for Z-DNA. The representative cylinder is clearly less porous than for B-DNA (*panel a1*): there is less room for the solute ions between the axis and the charged cylindrical surfaces that represent the phosphates. This leads to a larger value of the electrostatic potential, V, and of the cation concentration (*panel a2*), which is proportional to $\exp(zeV/kT)$. In mixed salt (*panel b*), the charge contribution of magnesium is 13.1%. It is larger than in the case of B-DNA, as mentioned in the previous section.

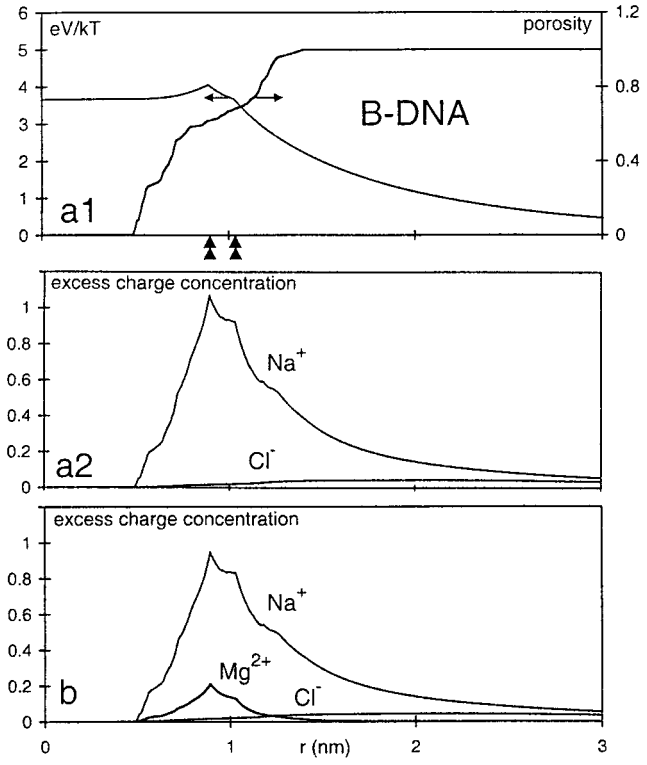

FIGURE 7 Radial distributions around the cylinder representing B-DNA. (*a1*) B-DNA in 50 mM monovalent salt solution. The electrostatic potential is in units of kT/e. A value of 3 corresponds to a 20-fold enhancement of the monovalent cation concentration. The porosity is the volume fraction accessible to ions (radius 0.235 nm). The position of the charged phosphate oxygens is indicated by arrowheads. (*a2*) B-DNA in 50 mM monovalent salt solution. The excess cylindrical charge concentration over the concentration at large, due to sodium accumulation and chlorine depletion. The unit is charge/phosphate/nm. The sum of the areas under the curves is equal to 1. (*b*) DNA in mixed salt solution: 50 mM monovalent and 0.1 mM divalent cations. The divalent cation contribution is enhanced at high electrostatic potential, i.e., at small radii.

COMPARISON WITH EXPERIMENTS

We now show that the theory explains in straightforward fashion the principal effects of many monovalent, divalent, and trivalent cations, including the surprising features presented in Table 1 and in Figs. 2 and 3. The semi-quantitative

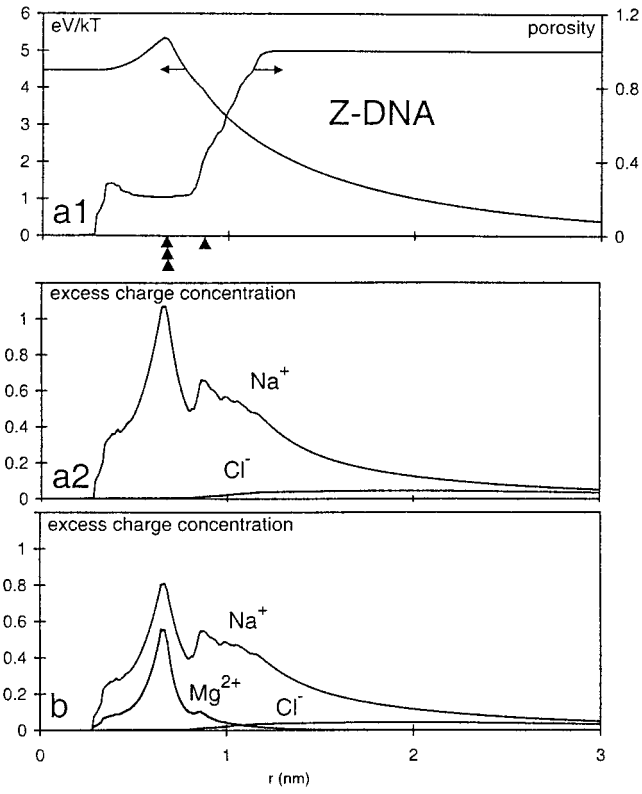

FIGURE 8 Companion figure to Fig. 7, for Z-DNA. Note the lower porosity and larger electrostatic potential (*panel a1*), and the larger partial charge of magnesium (*panel b*).

agreement between theory and experiment, obtained without any adjustable parameter, is also displayed in Fig. 9.

poly[d(G-C)], poly[d(G-m^{5}C)], and partially methylated polymers

The most obvious result of the theory is the straightforward explanation of the large difference in the observed response to magnesium of the B-Z transition between poly[d(G-C)] and poly[d(G-m^{5}C)] (Table 1). The difference is ascribed to the modest difference (0.44 kJ/phosphate) in the NFED. This term does not involve any particular interaction of the z-valent ion with the polyelectrolyte. It is not adjustable, being taken from a prior measurement of the total free energy difference between the B and Z forms in 100 mM NaCl (Peck and Wang, 1983; Zacharias et al., 1988). As a consequence of this difference, the stable form of poly[d(G-m^{5}C)] in low concentrations of divalent salt is the Z form, whereas it is the B form for poly[d(G-C)] (Fig. 4).

The disproportionate effect of methylation in partially methylated polymers (Behe and Felsenfeld, 1981) is also explained by the theory. We make the plausible assumption that the NFED is linearly related to the degree of methylation. By reference to Fig. 4, the positions of the −NFED horizontals for 30% and 70% methylation would then be at 0.54 and 0.36 kJ below the 1.86 kJ/mol position, so that these species should behave qualitatively like the fully methylated species in mixed divalent/monovalent salt. For a sodium concentration of 50 mM, the computed critical concentrations of divalent ions are respectively 5 and 1 mM, as compared to the experimental values, 20 and 1 mM.

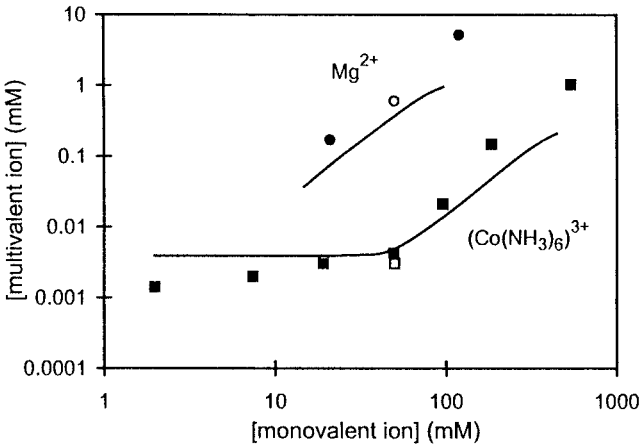

FIGURE 9 The B-Z transition of poly[d(G-m^{5}C)] in mixed salt solutions. The data points for Mg^{2+} (●) and $Co(NH_3)_6^{3+}$ (■) are from Fig. 3, for the case of 70 μM DNA phosphate. The plot is of total, rather than free, ionic concentrations. The solid lines are from the present theory, with no adjustable parameter. The empty symbols, ○ and □, correspond to data from Table 1.

Cation competition

The addition of monovalent salt to a divalent salt solution of poly[d(G-m^{5}C)] drives the Z to B transition by competition with the divalent cations in the sheath. A similar behavior is predicted for both poly[d(G-C)] and poly[d(G-m^{5}C)] in the case of trivalent and more highly charged cations. These transitions provide experimental tests of the theory.

Cation concentrations

The theoretical z-valent cation concentration for the B-Z transition in mixed salt is proportional to the z power of the monovalent concentration. This is in agreement with many observations, for instance with the variation of the critical concentrations of magnesium or cobalt hexammine as a function of monovalent ion concentration. Theory and experiment are compared in Fig. 9. (Because total, rather than free, ionic concentrations are plotted, the plot levels off at low total concentrations of cobalt hexammine. See the next paragraph.) The agreement between theory and experiment is rather good, particularly when one considers that neither the slope nor the position of the theoretical curves is adjustable.

The computed critical cobalt hexammine concentrations in 50 mM sodium are 1.2 μM for poly[d(G-m^{5}C)] and 70 μM for poly[d(G-C)]. These values may be surmised by interpolation in Fig. 6 *a*. They are in qualitative agreement with the experimental ones in Table 1, respectively 3 and 30 μM. Agreement is also quite good regarding the transition of poly[d(G-m^{5}C)] in mixed magnesium/sodium salt, as shown in Fig. 9, and correspondingly by the construction in Fig. 5 *a,* which shows the transition occurring for 0.6 mM magnesium and 67 mM sodium.

Constant sheath composition

At the transition in mixed salt, the theoretical sheath composition is independent of the monovalent salt concentration. This is in good agreement with the data in Fig. 3 *b*. As noted above, the sheath compositions of the B and Z forms differ (Figs. 5 *c* and 6 *c*), and the experimental value is their average. Previously, the constant sheath composition had been considered evidence for a fixed number of special affinity sites in one of the DNA forms (Chen et al., 1984).

Value of the multivalent-ionic charge in the sheath

The value derived from Fig. 5 *c* for divalent ions and poly[d(G-m^{5}C)] is 0.24, in good agreement with the experimental value for magnesium, 0.20 (Chen et al., 1984). For cobalt hexammine, Fig. 6 *c* gives 0.12 for poly[d(G-m^{5}C)], as compared to the experimental value, 0.07 (Chen et al., 1984). (These values correspond also to the left-hand part of Figs. 3 *B* and 9.) For poly[d(G-C)], the theoretical value is

0.45 (Fig. 6 *c*). However, no measurement is available for comparison. We mention again the lack of measurements of the individual charge fractions for the B and Z forms.

The B-Z transition in pure salt

The theory predicts a B-Z transition in pure monovalent salt for both polymers (points C1 and mC1, Fig. 4) and a transition in pure divalent salt only for poly[d(G-C)] (point C2), as observed. Quantitatively, the agreement is good for mC1 (0.75 M predicted, 0.7 observed) and fairly good for C1 (3.7 M predicted, versus 2.4 observed) but not for C2 (0.1 M predicted versus 0.7 in pure magnesium). However, it is clear from the figure that a slight change in the −NFED of poly[d(G-C)] would have a large effect on the monovalent concentration at C2. One also notes that substitution of Ca^{2+} for Mg^{2+} brings the experimental critical concentration to 0.1 M instead of 0.7 M.

One might consider addressing such differences by other ion-specific properties than charge, for instance the ionic radius. But the point stressed here is the explanation of the general features of the B-Z transition by a theory that ignores such specific features and which uses no adjustable parameter.

Temperature dependence

The theory provides a simple explanation for the bewildering results of Fig. 2, as follows. Let us assume that the value of −NFED increases with temperature. (The variation of the dielectric constant of water, from 88 at 0°C to 56 at 100°C, could perhaps be a contributing factor.) As the −NFED line is raised (Fig. 4), the critical magnesium concentration at C2 (for poly[d(G-C)] varies in a qualitatively similar fashion to Fig. 2 *a*. Comparison of Figs. 2 *a* and 4 shows that the required variation is ~2.6 J/deg. Furthermore, it is clear from Fig. 4 that the variation of −NFED affects the critical concentration much more in the case of divalent than in the case of monovalent cations. For poly[d(G-m^5C)], the effect on mC1 explains the negative slope of the critical sodium concentration in Fig. 2 *b, right-hand panel*.

The positive slopes in the left-hand panel of Fig. 2 *b*, which refers to mixed salt solutions, are explained by reference to Figs. 5 *a* and 6 *a*, which show that the critical monovalent ion concentrations at mC1 and at mC(mix) must move in opposite directions when the −NFED line is moved up. These trends in Fig. 2 *b* had been considered paradoxical.

We similarly explain the relative slopes for divalent and trivalent ions. The experimental slopes are in the ratio of 2 to 3 (Fig. 2 *b*). This is once again the $n_z/n_1{}^z$ phenomenon. The theoretical slopes are those of the EFED in mixed salt at point mC(mix). Comparison of Figs. 5 *a* and 6 *a* shows that they are indeed in roughly the same ratio. The case of spermine^{4+} in Fig. 2 *b* is not amenable to the same analysis because the total quantity of spermine in these experiments is so low that the free concentration is unknown and may vary with temperature.

Screening favors the Z form

Whether one uses large concentrations of monovalent ions or replaces monovalent by multivalent cations in the sheath, the result is usually the same: screening favors the Z form. This observation is so pervasive that it is easily taken for granted. It is nevertheless a strong point in favor of the present theory, which explains it in straightforward fashion, by the easier screening of the B form due to the immersion of the phosphates (or of the uniform cylindrical charge layers that represent them), so that further screening favors the Z form more than the B form.

OTHER CATIONS

The electrostatic theory provides an explanation of the B-Z transitions in sodium, magnesium, and cobalt hexammine, including (Table 1) the effects of cytosine methylation: a considerable effect on the critical magnesium concentration, and a modest effect on that of cobalt hexammine. These are the cations whose effect on the B-Z transition has been the most extensively studied. They are rather inert and therefore good candidates for a nonspecific, purely electrostatic interpretation.

A spectacular success of the theory is the explanation of the low critical values of the cobalt hexammine concentration and of the small cobalt/phosphate ratio at the transition. Such numbers had always been considered in the light of chemical interactions: they could not originate from pure electrostatics. The single most important feature of the present theory for the electrostatic explanation of these numbers is the near-invariance of the EFED in low salt (Fig. 4). This is a property of the EFED in the nonlinear regime between two highly charged surfaces that differ either in their charge or, as in the present case, in the screening of their charge.

We now turn to measurements of the B-Z transition in solutions of other cations, some of which behave similarly to those of Table 1, whereas others may show effects of ion specificity. Unfortunately, the measurements are often less complete than those for the ions in Table 1. Furthermore, left-handed DNA comes in more forms than one, with differences in circular dichroism spectrum and/or tendency to aggregate (van de Sande et al., 1982). Depending on the Z-inducing agent (cations, alcohols, high temperature), a different form may be favored.

Cations to which the electrostatic theory directly applies

Let us start with cations that behave similarly to the canonic cations, and whose properties are therefore explained by a theory devoid of ion-specific properties, except charge. All the monovalent alkaline cations drive a B to Z transition in high salt, at concentrations ranging from 2.3 M for NaCl to 4.7 M for CsCl (Soumpasis et al., 1987). The case of lithium involves an anomalous right-handed form (Behe et al., 1985). Like magnesium, the alkaline-earth cations Ca^{2+} and Ba^{2+} drive a high-concentration transition in poly[d(G-C)] (respectively at 0.1 and 0.04 M) and a low-concentration one in poly[d(G-m^{5}C)] (Behe and Felsenfeld, 1981). The hexammines of ruthenium (Thomas and Messner, 1988) and rhodium (Thomas and Thomas, 1990) have the same effect as cobalt hexammine on the two polymers.

Transition metal cations

The divalent ions of zinc, copper, manganese, cobalt, and nickel drive the B to Z transition of poly[d(G-m^{5}C)] at low concentrations, comparable to the critical concentration of magnesium. But, in contrast to magnesium, all of these ions except Cu^{2+} drive the transition of poly[d(G-C)] at low concentrations, typically only 10 times larger than for the transition of the methylated polymer (van de Sande et al., 1982; Woisard et al., 1985).

The usual interpretation is that the transition ions, in contrast to magnesium and the other alkaline earths, tend to coordinate to guanosine N7, and that since this group is more accessible in the Z than in the B structure, the interaction is stronger in the Z form. It is indeed observed that transition metal ions (and even alkaline-earth ions) coordinate to the N7 position of B-DNA in solution (Schoenknecht and Diebler, 1993) and of Z-DNA in the crystal (Gessner et al., 1985; Gao et al., 1993). The data are suggestive, but they do not provide a detailed description, for a number of reasons: comparisons of coordination of a given ion to B-DNA and to Z-DNA are not available; coordination in the crystal and in solution may be different; and multiple modes of coordination are often observed.

We now show that a chemical affinity of the transition metal ion for N7 (as opposed to none for magnesium) explains the quite different responses of poly[d(G-C)] to these ions. The affinity makes a supplementary contribution to the free energy, above and beyond the NFED determined in monovalent ions and the (electrostatic) EFED, which in our theory is the same for all divalent ions. Referring to Fig. 4, we see that the EFED in pure divalent salt is at most ~0.1 kJ/phosphate higher than the −NFED line of poly[d(G-C)]. If the new contribution is equal to or larger than this, the FED becomes negative, and the stable form in pure salt of the transition metal becomes the Z form, even at low concentrations. Since neither the experimental nor the theoretical values can claim 0.1 kJ/phosphate accuracy, we shall arbitrarily raise the minimum requirement to 0.2 instead of 0.1 kJ/phosphate. The situation is now similar to that of poly[d(G-m^{5}C)] in magnesium (Fig. 5): addition of monovalent salt will drive a Z to B transition. Correspondingly, starting from a solution in monovalent salt, addition of small amounts of the transition metal ion will cause a transition from the B to the Z form. Once again, the effect is enhanced by the near-equality of the EFED in divalent salt and of the value of −NFED for poly[d(G-C)] (Fig. 4).

An interesting feature of the problem is that, due to the different number of divalent ions in the sheath, the introduction of chemical affinity will favor the Z form, even if the affinities are the same for the B and Z forms: the difference is "built in" the polyelectrolyte electrostatics! Thus, the electrostatic theory provides a straightforward interpretation of the observation that the Z form is generally favored by transition metal ions more than by the alkaline earths.

The free energy of coordination of the transition ion is the product of the supplementary free energy per phosphate (we have assumed 0.2 kJ) by the number of phosphates per coordinated ion. We make the crude assumption that half of the transition metal ions in the sheath are bound. The free energy difference related to binding, bFED is, per phosphate:

$$\mathrm{bFED} = (1/2)(n_Z W_Z - n_B W_B) \qquad (10)$$

where n_Z is the number of transition metal cations in the sheath per phosphate and W_Z is the binding free energy per cation in the Z form, with corresponding definitions for the B form.

For instance, in mixed sodium/nickel solutions the B-Z transition of poly[d(G-C)] occurs for a ratio of 1 Ni^{2+} ion for 8 phosphates (Schoenknecht and Diebler, 1993), comparable to the number of magnesium ions at the transition in poly[d(G-m^{5}C)], where this corresponds to 0.26/2 and 0.18/2 magnesium ions per phosphate in the Z and B sheaths, respectively (Fig. 5 *c*). We use these values for n_Z and n_B. If we neglect the possible difference in the binding free energies to the B and Z forms, and take bFED = −0.2 kJ, Eq. 10 gives $W_Z = -10$ kJ/nickel cation. Or we may assume that W_Z is 2 kJ less than W_B, in which case we get −5.5 and −3.5 kJ/cation for W_B and W_Z, respectively. The corresponding dissociation constants are given by $\exp(-W/kT)$, with $kT = 2.5$ kJ at room temperature.

These considerations show that the contrasting effects of transition metal ions and of magnesium on the B-Z equilibrium of poly[d(G-C)] may be explained by coordination of the former ions to N7, and that this ion-specific effect requires only modest free energies of coordination, comparable to those measured for binding to neutral nucleosides (Izatt et al., 1971). The latter inform on ion-base interactions, in contrast with binding to bases (without the sugar moiety) or to ionized nucleosides, or with binding to nucle-

otides where the effects of phosphate are important, or with association to polynucleotides, which are affected by polyelectrolyte effects. The free energies are small enough to give modest differences with magnesium in the case of poly[d(G-m^{5}C)], as observed. We stress again that it is the coincidental near-equality of EFED in divalent salt and −NFED that gives visibility to the interaction of transition metals with DNA in the particular case of poly[d(G-C)].

CONCLUSION

The B-Z transition is sensitive to a variety of factors, such as methylation of cytidine, modification of solvent composition, or the addition of multivalent ions in small concentrations. Furthermore, the different actors may act synergistically. Despite their diversity, all of these factors operate through a single property of the electrostatic free energy of highly charged polyelectrolytes in low salt: its variation as the *logarithm* of salt concentration. As a result, the electrostatic free energy *difference* in pure salt is nearly independent of salt concentration. In such a condition, a slight modification of the *nonelectrostatic* free energy difference may change the relative stability of the two forms over a large range of salt concentrations. The equilibrium between the B and Z forms is therefore sensitive to minute variations of parameters and of their combinations, such as the difference in the effects of magnesium acting on poly[d(G-C)] and on poly[d(G-m^{5}C)]. This contrasts with the linear case (weakly charged polyelectrolytes), where the free energy difference increases monotonously as the salt concentration is reduced, so that a modest change in the NFED may be compensated by a proportionate change in ionic concentrations.

To summarize, a general, unified explanation of the principal features of the B-Z transition requires no more than a Poisson-Boltzmann theory, using cylindrical models of DNA whose principal property is that they reflect the better immersion of the B-DNA phosphate charges into the solution. The theory explains the effect of micromolar and strongly substoichiometric concentrations of cobalt hexammine without assuming any chemical interactions between the cation and DNA.

Chemical interactions affect the B-Z equilibrium. It is interesting that they may do so even if they are the same in the B and Z forms. As an example of a chemical interaction, the coordination of transition ions to N7 of guanine explains the difference between their effect and that of magnesium on the B-Z equilibrium of poly[d(G-C)]. It is noteworthy that the required coordination free energy is again modest. We believe that the properties of the B-Z transition, and the theory used here to explain them, illustrate general features of the structural physical chemistry of nucleic acids.

REFERENCES

Anderson, C. F., M. T. Record, and P. A. Hart. 1978. Sodium-23 NMR studies of cation-DNA interactions. *Biophys. Chem.* 7:301–316.

Behe, M., and G. Felsenfeld. 1981. Effects of methylation on a synthetic polynucleotide: the B-Z transition in poly(dG-m5dC) · poly(dG-m5dC). *Proc. Natl. Acad. Sci. USA.* 78:1619–1623.

Behe, M., G. Felsenfeld, S. Chen Szu, and E. Charney. 1985. Temperature-dependent conformational transitions in poly(dG-dC) and poly(dG-m5dC). *Biopolymers.* 24:289–300.

Chen, H. H., M. Behe, and D. C. Rau. 1984. Critical amount of oligovalent ion binding required for the B-Z transition of poly(dG-m^{5}dC). *Nucleic Acids Res.* 12:2381–2389.

Demaret, J. Ph., and M. Guéron. 1993. Composite cylinder models of DNA: application to the B-Z transition of DNA. *Biophys. J.* 65: 1700–1713.

Fenley, M. O., G. S. Manning, and W. K. Olson. 1990. A numerical counterion condensation analysis of the B-Z transition of DNA. *Biopolymers.* 30:1205–1213.

Frank-Kamenetskii, M. D., A. V. Lukashin, and V. V. Anshelevich. 1985. Application of polyelectrolyte theory to the study of the B-Z transition in DNA. *J. Biomol. Struct. Dyn.* 3:35–42.

Gao, Y., M. Sriram, and A. H. J. Wang. 1993. Crystallographic studies of metal ion- DNA interactions: different binding modes of cobalt(II), copper(II) and barium(II) to N^7 of guanines in Z-DNA and a drug-DNA complex. *Nucleic Acids Res.* 21:4093–4101.

Gessner, R. V., G. J. Quigley, A. H. Wang, G. A. van der Marel, J. H. van Boom, and A. Rich. 1985. Structural basis for stabilization of Z-DNA by cobalt hexammine and magnesium cations. *Biochemistry.* 24:237–240.

Grahame, D. C. 1947. The electrical double layer and the theory of electrocapillarity. *Chem. Rev.* 41:441–501.

Guéron, M., and J. Ph. Demaret. 1992a. Polyelectrolyte theory 4. Algebraic expression for the Poisson-Boltzmann free energy of a cylinder. *J. Phys. Chem.* 96:7816–7820.

Guéron, M., and J. Ph. Demaret. 1992b. A simple explanation of the electrostatics of the B-Z transition of DNA. *Proc. Natl. Acad. Sci. USA.* 89:5740–5743.

Guéron M., and J. L. Leroy. 1982. Significance and mechanism of divalent-ion binding to transfer RNA. *Biophys. J.* 38:231–236.

Guéron, M., and G. Weisbuch. 1979. Polyelectrolyte theory 2. Activity coefficients in Poisson-Boltzmann, and in condensation theory. The polarizability of the counterion sheath. *J. Phys. Chem.* 83:1991–1998.

Guéron, M., and G. Weisbuch. 1980. Polyelectrolyte theory. 1. Counterion accumulation, site-binding, and their insensitivity to polyelectrolyte shape in solutions containing finite salt concentrations. *Biopolymers.* 19:353–382.

Heus, H. A., and A. Pardi. 1991. Nuclear magnetic resonance studies of the hammerhead ribozyme domain. Secondary structure formation and magnesium ion dependence. *J. Mol. Biol.* 217:113–124.

Izatt, R. M., J. J. Christensen, and J. H. Rytting. 1971. Sites and thermodynamic quantities associated with proton and metal ion interaction with ribonucleic acid, deoxyribonucleic acid, and their constituent bases, nucleosides and nucleotides. *Chem. Rev.* 71:439–480.

Katahira, M., M. H. Kim, T. Sugiyama, Y. Nishimura, and S. Uesugi. 1998. Two metal-binding sites in a lead ribozyme bound to competitively by Pb^{2+} and Mg^{2+}: induced structural changes as revealed by NMR. *Eur. J. Biochem.* 255:727–733.

Klement, R., D. M. Soumpasis, and T. M. Jovin. 1991. Computation of ionic distributions around charged biomolecular structures: results for right-handed and left-handed DNA. *Proc. Natl. Acad. Sci. USA.* 88: 4631–4635.

Legault, P., C. G. Hoogstraten, E. Metlitzky, and A. Pardi. 1998. Order, dynamics and metal-binding in the lead-dependent ribozyme. *J. Mol. Biol.* 284:325–335.

Leroy, J. L., and M. Guéron. 1977. Electrostatic effects in divalent ion binding to tRNA. *Biopolymers.* 16:2429–2446.

Leroy, J. L., and M. Guéron. 1981. The distance of manganese to phosphorus atoms of polynucleotides, and dynamics of binding. *Biochimie.* 63:815–819.

Leroy, J. L., M. Guéron, G. Thomas, and A. Favre. 1977. Role of divalent ions in folding of tRNA. *Eur. J. Biochem.* 74:567–574.

Manning, G. S. 1969. Limiting laws and counterion condensation in polyelectrolyte solutions. I. Colligative properties. *J. Chem. Phys.* 51: 924–933.

Manning, G. S. 1978. The molecular theory of polyelectrolyte solutions with applications to the electrostatic properties of polynucleotides. *Q. Rev. Biophys.* 11:179–246.

Misra, V. K., and B. Honig. 1996. The electrostatic contribution to the B to Z transition of DNA. *Biochemistry.* 35:1115–1124.

Peck, L. J., and J. C. Wang. 1983. Energetics of the B-to-Z transition in DNA. *Proc. Natl. Acad. Sci. USA.* 80:6206–6210.

Pohl, F. M. 1983. Salt-induced transition between two double-helical forms of oligo(dC-dG). *Cold Spring Harbor Symp. Quant. Biol.* 47:113–118.

Pohl, F. M., and T. M. Jovin. 1972. Salt-induced co-operative conformational change of a synthetic DNA: equilibrium, and kinetic studies with poly(dG-dC). *J. Mol. Biol.* 67:375–396.

Sági, J., A. Szemzö, L. Ötvös, M. Vorlicková, and J. Kypr. 1991. Destabilization of the duplex, and the high-salt Z-form of poly(dG-methyl5dC) by substitution of ethyl for the 5-methyl group. *Int. J. Biol. Macromol.* 13:329–336.

Schoenknecht, T., and H. Diebler. 1993. Spectrophotometric and kinetic studies of the binding of Ni^{2+}, Co^{2+}, and Mg^{2+} to poly(dG-dC) · poly(dG-dC). Determination of the stoichiometry of the Ni^{2+}-induced B → Z transition. *J. Inorg. Biochem.* 50:283–298.

Simorre, J. P., P. Legault, A. B. Hangar, P. Michiels, and A. Pardi. 1997. A conformational change in the catalytic core of the hammerhead ribozyme upon cleavage of an RNA substrate. *Biochemistry.* 36: 518–525.

Singleton, C. K., J. Klysik, S. M. Stirdivant, and R. D. Wells. 1982. Left-handed Z-DNA is induced by supercoiling in physiological ionic conditions. *Nature.* 299:312–316.

Soumpasis, D. M., M. Robert-Nicoud, and T. M. Jovin. 1987. B-Z conformational transition in 1:1 electrolytes: dependence upon counterion size. *FEBS Lett.* 213:341–344.

Stirdivant, S. M., J. Klysik, and R. D. Wells. 1982. Energetic and structural interrelationship between DNA supercoiling and the right- to left-handed Z helix transitions in recombinant plasmids. *J. Biol. Chem.* 257: 10159–10165.

Thomas, T. J., and R. P. Messner. 1988. Hexammine ruthenium(III) chloride: a highly efficient promoter of the B-DNA to Z-DNA transition of poly-(dG-m5dC) · poly(dG-m5dC) and poly(dG-dC)) · poly(dG-dC). *Biochimie.* 70:221–226.

Thomas T. J., and T. Thomas. 1990. Conformational transitions of polynucleotides in the presence of rhodium complexes. *J. Biomol. Struct. Dyn.* 7:1221–1235.

van de Sande, J. H., and T. M. Jovin. 1982. Z* DNA, the left-handed helical form of poly[d(G-C)] in MgCl2-ethanol, is biologically active. *EMBO J.* 1:115–120.

van de Sande, J. H., L. P. McIntosh, and T. Jovin. 1982. Mn^{2+} and other transition metals at low concentration induce the right-to-left helical transformation of poly(d(G-C)). *EMBO J.* 1:777–782.

Wang, A. H. J., G. L. Quigley, F. J. Kolpak, J. L. Crawford, J. H. van Boom, G. van der Marel, and A. Rich. 1979. Molecular structure of a left-handed double helical DNA fragment at atomic resolution. *Nature.* 282:680–686.

Weisbuch, G., and M. Guéron. 1981. Polyelectrolyte theory. 3. The surface potential in mixed-salt solutions. *J. Phys. Chem.* 85:517–525.

Weisbuch, G., and M. Guéron. 1983. Une longueur d'échelle pour les interfaces chargées. *J. Physique.* 44:251–256.

Woisard, A., G. Fazakerley, and W. Guschlbauer. 1985. Z-DNA is formed by poly(dC-dG) and poly(dm5C-dG) at micro or nanomolar concentrations of some zinc(II) and copper(II) complexes. *J Biomol. Struct. Dyn.* 2:1205–1220.

Zacharias, W., T. R. O'Connor, and J. E. Larson. 1988. Methylation of cytosine in the 5-position alters the structural and energetic properties of the supercoil-induced Z-helix, and of B-Z junctions. *Biochemistry.* 27: 2970–2978.